

Article

Laser-Based Additive Manufacturing of Zirconium

Himanshu Sahasrabudhe and Amit Bandyopadhyay *

W. M. Keck Biomedical Materials Research Center, School of Mechanical & Materials Engineering,
Washington State University, Pullman, WA 99164-2920, USA; himsaha17@outlook.com

* Correspondence: amitband@wsu.edu; Tel.: +1-509-335-4862

Received: 12 January 2018; Accepted: 16 February 2018; Published: 7 March 2018

Abstract: Additive manufacturing of zirconium is attempted using commercial Laser Engineered Net Shaping (LENSTM) technique. A LENSTM-based approach towards processing coatings and bulk parts of zirconium, a reactive metal, aims to minimize the inconvenience of traditional metallurgical practices of handling and processing zirconium-based parts that are particularly suited to small volumes and one-of-a-kind parts. This is a single-step manufacturing approach for obtaining near net shape fabrication of components. In the current research, Zr metal powder was processed in the form of coating on Ti6Al4V alloy substrate. Scanning electron microscopy (SEM) and energy dispersive spectroscopy (EDS) as well as phase analysis via X-ray diffraction (XRD) were studied on these coatings. In addition to coatings, bulk parts were also fabricated using LENSTM from Zr metal powders, and measured part accuracy.

Keywords: additive manufacturing; zirconium metal; Laser Engineered Net Shaping (LENSTM); coating; 3D printing

1. Introduction

Additive manufacturing of zirconium (Zr) metal was done using the Laser Engineered Net Shaping (LENSTM) technique. Zirconium is commonly used in the nuclear, space, and aerospace industries due to its exceptional corrosion and oxidation resistance [1–4]. Zirconium has also found uses in the biomedical device industry for load-bearing implants due to its wear and corrosion resistance [5–7]. These applications utilize Zr metal in the form of bulk components. Besides these bulk components, zirconium is also a popular choice for coatings to enhance high temperature oxidation resistance. For coatings on titanium alloys, Zr is used to serve the dual purpose of oxidation resistance at high temperatures and maintain the structural integrity with Ti6Al4V components when used in compositionally graded structures with other alloys.

Zirconium is a highly reactive metal in molten state and in the open atmosphere in presence of oxygen and hydrogen. It is pyrophoric in powdered state. This requires a special inert atmosphere or high vacuum in furnaces and smelting plants to maintain the purity of the metal as well as prevent fire hazards. Furthermore, due to its enhanced chemical activity in molten state, it can also take a toll on the crucible materials. Thus, processing of zirconium parts can be cumbersome, which can cause wastage of the precious metal. Due to rapid work hardening and formation of a brittle oxide layer on the surface, metal forming practices such as wire drawing and rolling are also challenging for Zr metal. Multiple annealing–cold working cycles are necessary. Annealing and other heat treatment practices are difficult due to the affinity of zirconium to common gases like oxygen and hydrogen at higher temperatures [8]. Hence, these difficulties necessitate processes that can be used safely to fabricate Zr components in a single step without degrading the desired properties.

Additive manufacturing techniques, especially the direct energy deposition-based techniques have several advantages over traditional metallurgical practices. These advantages include 3D forming capability along with complex geometries, rapidly cooled microstructures, and the ability to form site

specific compositionally graded structures. Along with bulk fabrication capability, these methods can also be used for surface modification. Thus, zirconium metal can be utilized in the form of coatings and these coatings can be processed in a single step process. Compositionally graded structures of zirconium with other important metallic materials such as Ti-based alloys can also be designed and fabricated in one operation. It is also possible to carry out laser-assisted repair of existing structures using zirconium instead of fabricating completely new structures. This could lead to cost savings and efficient use of precious metals like zirconium. These direct energy-based techniques or, more specifically, laser-based additive manufacturing techniques are carried out in a controlled, inert environment with low levels of oxygen. Such environmental control prevents any detrimental oxidation as well as fire hazards. All of these combined features of the additive manufacturing techniques can thus simplify the processing of materials like zirconium as well as make the processing safer and more economical.

Laser engineered net shaping (LENSTM) is one such direct energy deposition-based additive manufacturing technique [9]. The LENSTM process is capable of fabricating near net shaped components, fabricating compositionally and structurally graded components, fabricating surface coatings and repairing existing components. Additive manufacturing via the LENSTM technique has been demonstrated previously for various specialty materials that were otherwise difficult to process owing to their higher melting temperature, phase stability, or high cooling rate requirements. These materials include NiTi alloys [10,11], tantalum as bulk and as coating [12,13], bulk metallic glass or bulk amorphous alloys [14,15], bimetallic structures or dissimilar metal bonding [16] and bulk porous structures [17,18]. Thus, a material of such high engineering importance as zirconium, if successfully processed using additive manufacturing techniques such as LENSTM, can open new opportunities in fabrication and utilization [19,20]. Shifting to additive manufacturing technique for making bulk parts and compositionally graded parts as well as coatings can also result in cost and weight savings in the structure [21]. Hence, it is necessary to investigate if a reactive metal like zirconium can be directly processed via the additive manufacturing route.

In the current research, Laser Engineered Net Shaping (LENSTM), a powder-based additive manufacturing technique, has been utilized for processing zirconium metal coating on Ti6Al4V alloy substrate in an argon atmosphere with low oxygen, low nitrogen, and low hydrogen content. The purpose of this first generation research was to understand feasibility of processing a reactive material like zirconium as a bulk part and as a coating, and understand the influence of different processing parameters on properties. Furthermore, any variation in the microstructure and the properties of the coatings with a blank laser scan on the surface after depositing the Zr coatings was also investigated. Microstructural analysis was done using scanning electron microscopy (SEM) and Energy Dispersive Spectroscopy (EDS) attached to an SEM. Phase analysis was carried out using X-ray diffraction. Hardness measurements were done on LENSTM processed Zr samples.

2. Experimental Procedure

2.1. Laser Engineered Net Shaping (LENSTM)

LENSTM is a powder-based additive manufacturing technique that allows fabrication of near net shape metallic components from computer-aided design (CAD) files. The LENSTM system has a focused, high-powered laser beam that melts metallic powders. The powder or mixtures of powders are carried in pressurized argon gas into the focal point of the laser. The stage on which the laser is focused moves in the X and the Y directions in a raster scanning fashion. The powder melts under the laser power, and rapidly solidifies. The CAD design dictates the raster scanning motion and deposits a single layer of the design. Once a first layer is deposited, the feed assembly moves up in the Z direction to deposit another layer in a similar raster scanning fashion. This continued layer-by-layer deposition, controlled by the CAD files and additional motion control files, subsequently fabricates a complete 3D geometry. The entire build assembly is enclosed in a glove box that is purged with high-purity

argon. The oxygen level is maintained below 10 ppm, and is continuously monitored using an oxygen sensor. The LENSTM has two powder feeders or hoppers. Both of these feeders can be simultaneously used to execute in situ alloying. The two hoppers can also be independently used in the same part design to form compositionally graded structures. The LENSTM system can also be used for fabrication of thermally graded structures. With the aid of the LENSTM working software, processing parameters such as laser power, raster scan speed, and powder feeding rates are optimized to achieve a thermal gradient during solidification [16–18].

2.2. LENSTM Processing of Zirconium

Zirconium powder with a size distribution between 44 µm and 149 µm (+325–100 Mesh) and purity of 99.98% was used for LENSTM processing (CERAC Specialty Materials, Milwaukee, WI, USA). The substrate or base plate material used was Ti6Al4V alloy (President Titanium, Hanson, MA, USA) of 99.999% purity. The substrate Ti6Al4V alloy plate was 3 mm thick. LENSTM processing was done at different machine parameters that are tabulated in Table 1. Various problems and processing issues associated with each processing attempt have also been described. From the various attempts carried out, the optimum laser power of approximately 450 W was used at a raster scan speed of 80 cm/min and powder feed rate of 16 g/min. Two different geometries were processed. To study the interface with Ti6Al4V alloy for X-ray diffraction, SEM-EDS analysis, and hardness testing, square-shaped samples with side length of 14mm were processed. Each of these LENSTM-deposited coatings was between 1.0 to 1.5 mm thick. In addition to this, some samples were laser scanned at 450W with no powder addition to remelt and solidify the initially deposited material. To demonstrate the 3D near net shape manufacturing capabilities of the LENSTM system, a cylindrical component with inner diameter 15.24 mm (0.50 inch), outer diameter 25.40 mm (1.00 inch) and height of 25.40 mm (1.00 inch) was designed. This part was built on Ti6Al4V alloy base plate with the same LENSTM parameters as other Zr processed parts. The glove box of the LENSTM system was kept purged with high purity argon and oxygen was kept below 10 ppm during the processing of the Zr components.

Table 1. Different processing parameter tried and tested for LENSTM-based additive manufacturing of zirconium metal.

Power (W)	Speed (cm/min)	Powder Feed Rate (g/min)	Observed Processing Problems	Comments
~475—Maximum power available	100	~16	Large heating, sample remains red hot, slow cooling/solidification	Large heating will eventually cause cracking. Small coatings can be processed but large parts will not build
	60		Even more heating due to reduced speed. Globulation and agglomeration at laser focal point/melt pool to high feed rate and slow speed and high power.	
~435	100	~16	No excessive heating as compared to 475 W power. Speed seems to be a bit too fast for dense part	Power of ~450 W and speed of ~80 cm/min seems to be the ideal setting. Lower power settings have still to be tried.
	60		Slightly more heating since speed is only 60% of the previous trial at 435 W	
~400	100	~16	Feeling that powder is not getting enough heat and not “laying down” in thick enough layers	Power is too low. Speed will have to be drastically reduced to ensure complete melting of particles and avoid porosity. This can cause coarse microstructures and longer build times.
	60		More deposition but melt pool still appears cold for the feed rate, may cause extensive porosity and fragile part.	

2.3. Characterization of LENSTM Processed Zr Part

The square shaped samples fabricated by LENSTM were cut transversely using a low speed diamond saw. Cross-sections were then wet ground starting at 120 grit SiC paper subsequently to 1200 grit. Final polishing was done on alumina suspension in deionized water of size 1, 0.3, and 0.05 µm. Similar grinding and polishing was also done on the top deposited surface to make samples for X-ray

diffraction (XRD) analysis. All the samples used in XRD analysis were of the same thickness and surface finish. After polishing samples were cleaned in an ultrasonic bath in 100% ethanol at room temperature for 15 min and finally blow-dried in warm air.

The cross-sections were etched using Kroll's reagent (92 mL DI water, 6 mL HNO₃, 2 mL HF) for 30 s swabbing time. Samples were then analyzed in a scanning electron microscope (FEI Quanta 200, FEI Inc., Hillsboro, OR, USA) and SEM (FEI Sirion FEI Inc., Hillsboro, OR, USA) equipped with Energy Dispersive Spectra detector (EDAX Inc., Mahwah, NJ, USA). X-ray diffraction analysis was performed using a Siemens D-500 Kristalloflex D5000 Diffractometer (Siemens AG, Karlsruhe, Germany) with Cu K α radiation using a Ni filter between 20 and 80 degrees.

2.4. Microhardness Measurements

Microhardness measurements were performed on the cross sections of the LENSTM-processed Zr samples using a Shimadzu HVM-2 microhardness tester (Tokyo, Japan) equipped with a Vicker's diamond indenter. Hardness tests were performed before etching the samples with Kroll's reagent. The load applied was 100 g (0.98 N) and dwell time was 15 s for all as processed and laser passed Zr samples. Hardness values were recorded along the depth of the Zr, into the interface with Ti6Al4V substrate. Multiple hardness tests were performed at each depth for statistical certainty of the data.

3. Results

3.1. Process Optimization

Table 1 shows results from different attempts of processing Zr using LENSTM. The main parameters that could be controlled were the laser power, the raster scanning speed and the federate of the powder. While changing these parameters to get the most ideal build quality, the design of the files, the layer thickness and the raster scans of every layer were kept constant. The highest available laser power of 475 W caused excess heating of the Zr powder. Powder feed rate was kept constant in these attempts and the speed varied from 100 cm/min to 60 cm/min. At the slower speed, the melt pool was very large and build quality looked poor due to the formation of large globule of molten metal. At a faster speed this problem persisted. In attempting to build the larger cylindrical component, the initially deposited layers appeared red hot indicating excessive heating and delayed solidification. The laser power was then reduced to 435 W for the next set of samples. The speed was again varied between 100 cm/min and 60 cm/min, and powder feed rate was kept constant at 16 gm/min. This level of power appeared to suit the processing of Zr metal. The layers appeared dense at slower speed of 60 cm/min as compared to the speed of 100 cm/min. Power setting lower than 435 W was also tried. At the laser power of 400 W, it was observed that the melting of the incoming Zr powder was insufficient and the layers that were being deposited were not thick enough to fabricate a dense part. Attempt was made to deposit thicker layers by slowing down the raster scan and increasing the powder feed rate. However, this would only lead to more unmelted powder particles in the part. Based on these processing attempts, a laser power level of 450 W and a scan speed of 80 cm/min were selected to fabricate the coatings and the bulk part discussed in this research.

3.2. Microstructure and Phase Analysis

Figure 1a shows the low magnification image of LENSTM-deposited Zr in Ti6Al4V alloy with no laser pass on the surface. As visible from the SEM image, there was a clear interface between Ti6Al4V and the deposited Zr. However, there was no cracking or no visible delamination. Some porosity is present in the LENSTM-processed layers with pore size of $34.1 \pm 8.1 \mu\text{m}$. The total LENSTM-deposited Zr layer was found to be $1.76 \pm 0.12 \text{ mm}$. Observation of the SEM acquired microstructure in Figure 1 revealed the presence of two distinct zones in the deposited Zr region. The uppermost zone or Zone 1 was $1430.55 \pm 89.53 \mu\text{m}$ in thickness. Zone 2, above the interface with Ti6Al4V substrate, was $297.88 \pm 52.59 \mu\text{m}$ in thickness. The equiaxed grains in Zone 1 had an average grain size of

$0.69 \pm 0.07 \mu\text{m}$. This secondary phase along with the equiaxed grain can be observed in Figure 1b. In addition to this equiaxed structure, a secondary phase was observed. In the Zone 2, some patchy phases were also observed. SEM image in Figure 1c shows the transition from the equiaxed grained structure of Zone 1 to an elongated and marginally dendritic structure in Zone 2.

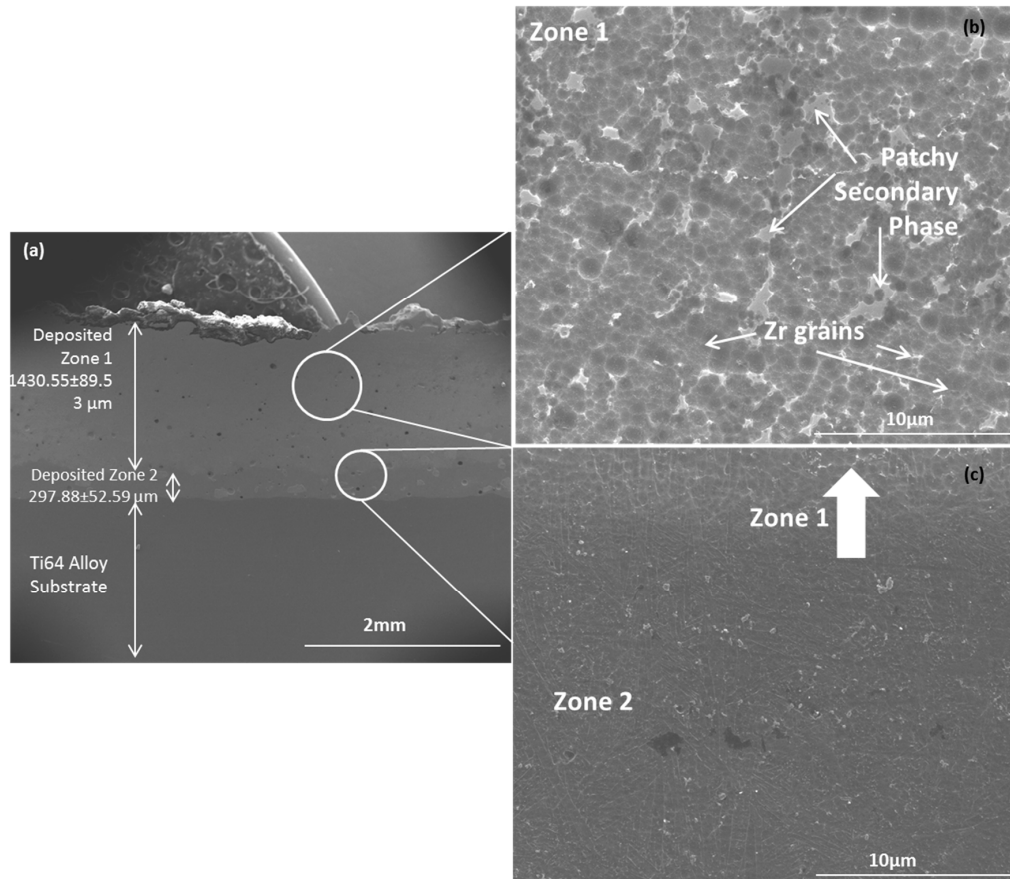


Figure 1. LENSTM-deposited Zr on Ti6Al4V (Ti64) alloy: (a) The coating; (b) uppermost zone or Zone 1; (c) transition to Zone 2 of the coating.

Figure 2a shows the structure of LENSTM-deposited Zr with a single laser pass on the surface after deposition. In this sample, there were three distinct zones visible above the interface with Ti6Al4V alloy unlike two zones observed in the samples without any laser pass on the surface. Overall, the thickness of the LENSTM-deposited zone in this sample was $1330.39 \pm 14.39 \mu\text{m}$. Porosity was also less, with an average pore size of $45.6 \pm 6.51 \mu\text{m}$. The different zonea, as well as their thicknesses, are shown in Figure 2a. The patchy phase that was observed in the sample with no laser pass was also seen in these samples after a laser pass. It was found to be more prominent and larger in size.

Higher magnification imaging of Zone 1 in the Zr region with one laser pass showed the spherical to equiaxed grained microstructure of Zr after LENSTM processing, as seen in Figure 2b. In the sample with one laser pass, the grain size remained unchanged and was $0.66 \pm 0.07 \mu\text{m}$. On top of these grains, some secondary phases were also seen. The lowermost zone immediately above the Ti6Al4V interface was also similar for both the sample. Hence, the laser scan on the surface after LENSTM deposition effectively created the extra zone. It created the Zone 1 (in Figure 2b) and the depth of this zone could be indicative of the effective depth of the laser remelting process. Figure 2c,d show the embedded phase that was found to be more prominent in the samples after laser pass. These particles shows a high contrast, irregular structure (Figure 2c), but had a smooth transition with the equiaxed phase around them (Figure 2d). Compared to the LENSTM-processed samples without any laser pass, the

secondary phase appeared to be less distributed and more agglomerated; the phase was larger in size and not as widely spread for laser pass samples. These differences can be seen in Figure 3a,b.

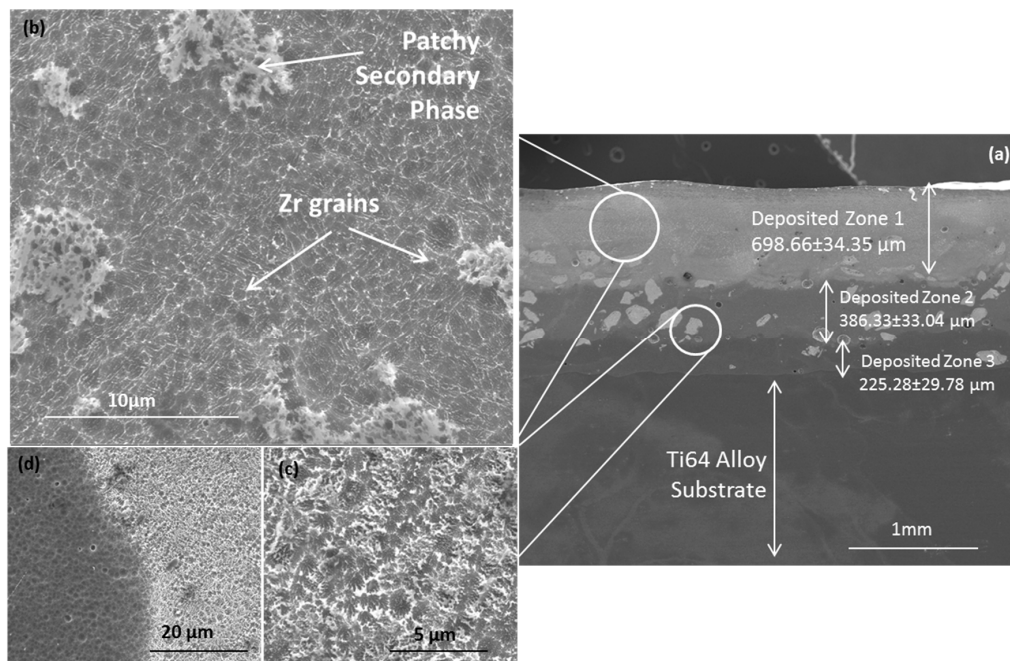


Figure 2. LENSTM-deposited Zr on Ti6Al4V (Ti64) alloy with One Laser Pass: (a) The coating; (b) uppermost region of the coating or Zone 1; (c) embedded particles in the coating; (d) the embedded phase and the phase surrounding it.

Figure 4a shows the phase analysis from the XRD data of the feedstock Zr powder. The feedstock powder prior to processing was found to contain only a single phase of Zr; only α phase was detected. Figure 4b,c show the results of the same for LENSTM-processed Zr on Ti6Al4V without and with a single laser pass, respectively. In both the cases, retention of α phase, hcp structure, of zirconium was prominent. Along with the α phase, the β phase with bcc structure was also noticed. From the Joint Committee on Powder Diffraction Standards (JCPDS) indexing file, the α (hcp) phase has lattice parameters of $a = 3.232 \text{ \AA}$, $c = 5.147 \text{ \AA}$, while the β (bcc) phase has lattice parameter of $a = 3.5453 \text{ \AA}$.

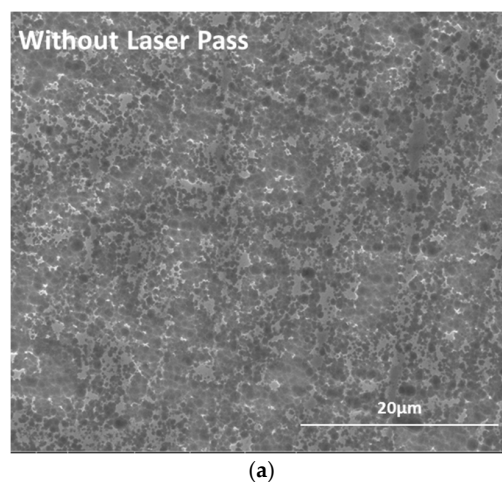


Figure 3. Cont.

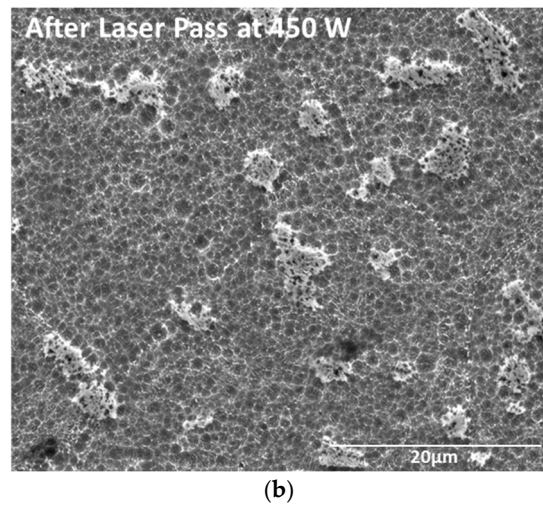


Figure 3. Zone 1 of the LENSTM-deposited Zr showing the secondary phase along with the equiaxed Zr grains (a) without a laser pass; (b) with one laser pass after deposition.

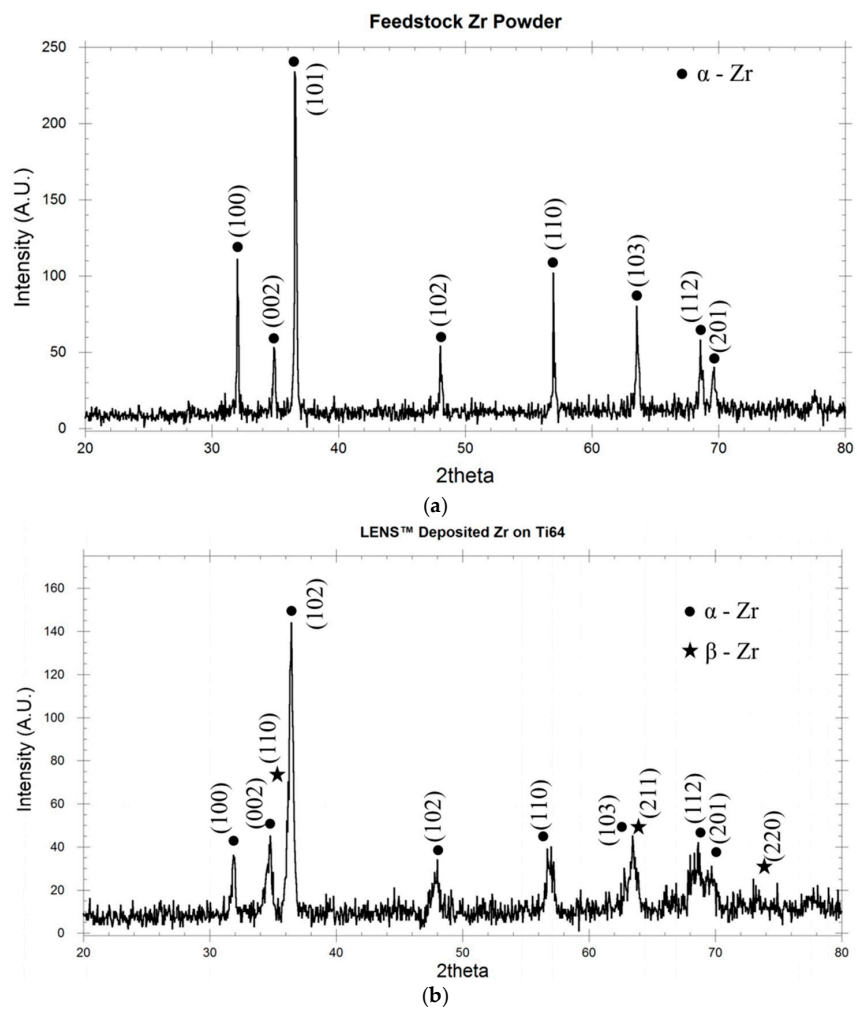


Figure 4. Cont.

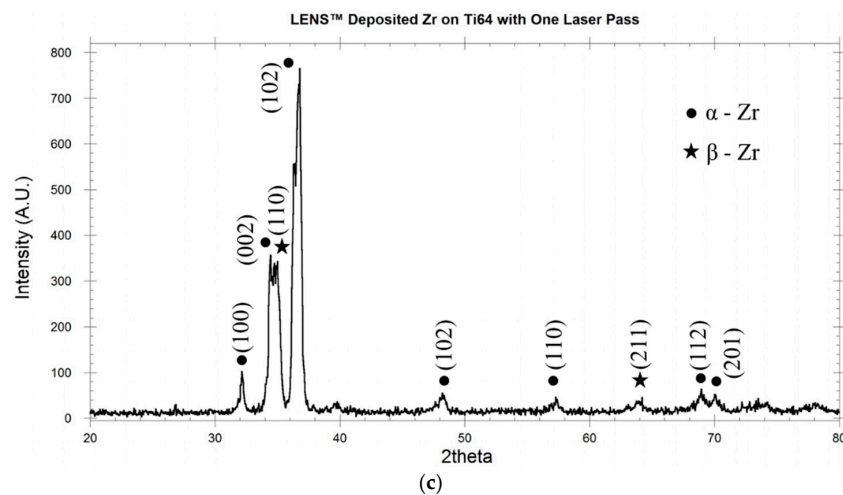


Figure 4. Phase analysis by XRD technique: (a) feedstock Zr powder; (b) LENSTM-processed Zr; and (c) LENSTM-processed Zr with one laser pass.

3.3. Compositional Analysis of LENSTM-Processed Zr on Ti6Al4V

Deposition of Zr metal on Ti6Al4V substrate using LENSTM led to the formation of two zone structures in the samples with no post-deposition laser scan, and three zone structures in the samples with one laser surface scan. In both cases, α as well as the β phases of Zr were formed. There was a large bright contrast phase in the interface region with more such phases occurring in the samples due to the addition of a laser pass. EDS was employed for two purposes: (i) to understand the dilution of Ti and Zr in each other; and (ii) to investigate the elemental composition of the phases observed at the interface. Figure 5 shows the elemental distribution of Ti, V, and Zr along the interface of the LENSTM-processed Zr on Ti6Al4V without any laser pass.

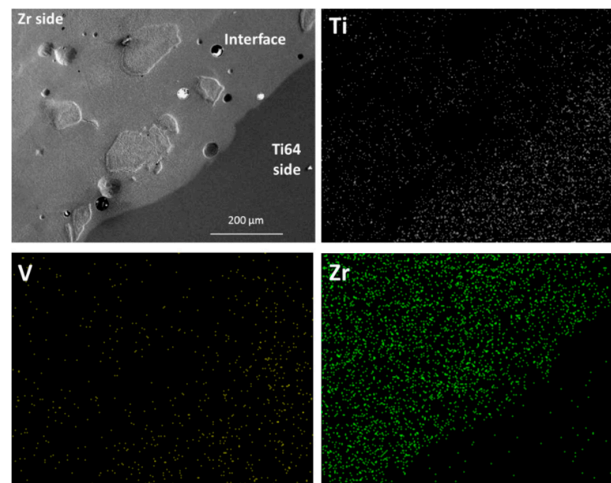


Figure 5. Elemental distribution along the interface of LENSTM-processed Zr on Ti6Al4V alloy.

Ti from the Ti6Al4V alloy substrate was found to dilute along the interface into the Zr interface region more than Zr. Vanadium from the Ti6Al4V alloy substrate was hardly detected on either side, while Al was detected even less due to its comparatively lower atomic weight. In the SEM images in Figure 5, large particles appear to be embedded in the interface region. These particles were observed in all the samples, irrespective of the post-deposition laser pass on the surface. Figure 6a,b show the EDS elemental mapping of one such particle in the interface. The embedded particles appeared to be

depleted in Ti and rich in Zr, as seen in Figure 6a. Even the particle that was very close to the Ti6Al4V alloy substrate, in Figure 6b, was depleted in Ti.

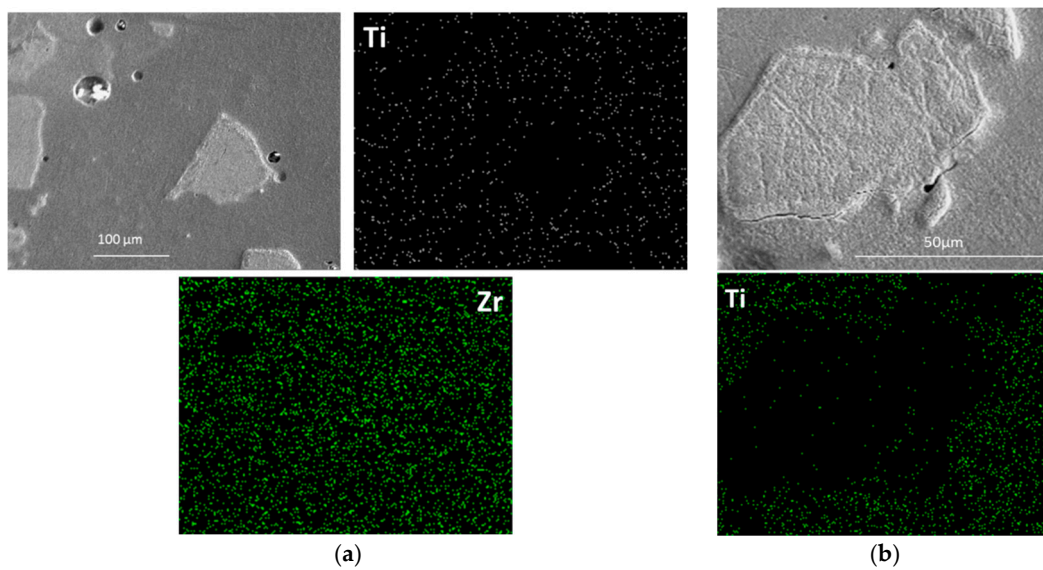


Figure 6. (a) Elemental distribution of the embedded particles; (b) similar particle at higher magnification.

3.4. Microhardness Measurement

Figure 7a,b shows the variation of the hardness of LENSTM-deposited Zr with the depth from the top surface of the Zr. From Figure 7a, it can be seen that the maximum hardness achieved in the Zr region after LENSTM deposition was 268 HV0.1. After a laser pass, the maximum hardness increased to 326 HV0.1. In both cases, this hardness gradually decreased into the Ti6Al4V substrate to a hardness of 240 HV0.1. The hardness values for both types of samples were not found to vary by a large amount, as seen in Figure 7.

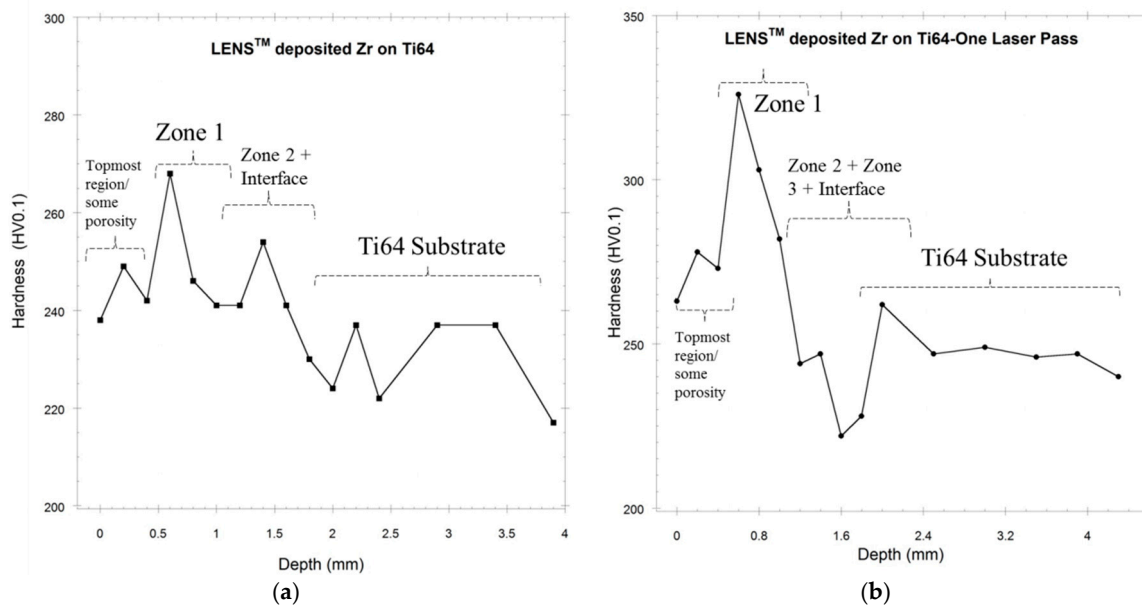


Figure 7. Hardness depth profile of LENSTM-deposited Zr on the Ti6Al4V (Ti64) alloy: (a) no laser pass; (b) with one laser pass.

3.5. Bulk Zirconium Part Fabrication

Figure 8 shows a tube structure made of zirconium using LENSTM. This part was designed with an inner diameter 15.24 mm, an outer diameter 25.40 mm, and a height of 25.40 mm. After LENSTM deposition, the “as-processed” outer diameter was 26.90 ± 0.42 mm. This measurement confirms a $5.90 \pm 1.64\%$ radial expansion during LENSTM deposition.

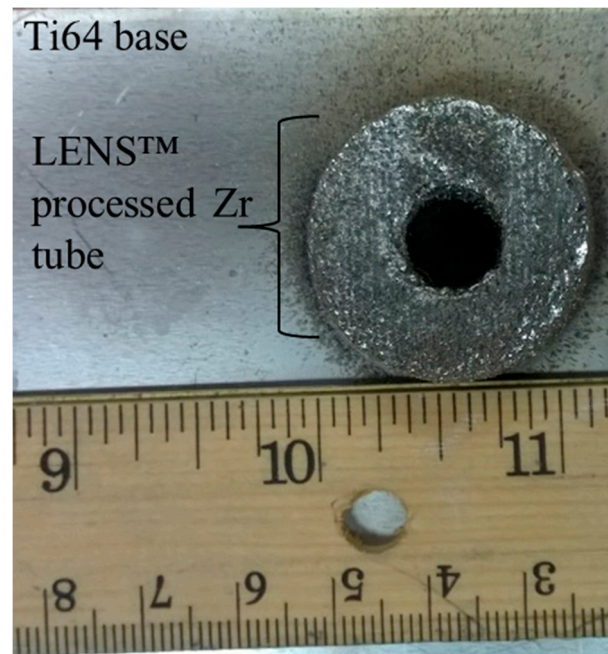


Figure 8. LENSTM-processed Zr cylindrical/tube geometry.

4. Discussion

Laser Engineered Net Shaping (LENSTM) is a powder-based additive manufacturing technique. It has several features such as controlled inert environment, focused high power laser, and in situ alloying and composite deposition. These features are ideal for the processing of specialty materials like superalloys and NiTi alloys, high melting point materials such as tantalum as well as in the fabrication of specialized designs such as three-dimensional porous or bimetallic components. In the current research, zirconium, a reactive metal, was processed using the LENSTM technique on a Ti6Al4V alloy. Initial SEM scans revealed the presence of some porosity in spite of extensive process optimization. The parameters thus need to be further optimized for forming dense Zr coatings or 3D structures. Nevertheless, it was shown that Zr can be additively manufactured using a direct energy deposition technique such as LENSTM.

LENSTM processing of Zr produced a zoned microstructure. It consisted of equiaxed grains that were less than a micron in size. Some samples were subjected to a laser scan on the surface after initial LENSTM deposition. However, such a laser pass did not affect the grain size. In the samples without any laser pass, there were two distinct zones found in the Zr region. The top region had equiaxed grains, while the region beneath it and directly above the Ti6Al4V substrate had similar grain but with embedded particles, presumably of another phase of Zr. The samples that were laser-passed after initial deposition had an additional layer between the embedded phase layer and the top equiaxed grained layer. This layer also showed similar embedded particles. In both types of Zr depositions, there was a secondary, patchy phase seen along with the equiaxed grains. It seemed to agglomerate and spread more evenly after the laser pass on the surface.

Phase analysis of the LENSTM-deposited Zr samples showed the formation of both α and β phases of Zr. The feedstock powder was purely α (hcp) phase. However, the microstructure showed a single type of equiaxed grains in the upper regions. In the regions close to the interface, the secondary embedded phase was found. We hypothesize that the upper regions of the equiaxed grains in both types of samples are in the α -Zr phase. Near the regions closer to the Ti6Al4V substrate, owing to the stabilizing effect of Ti, there is β -Zr (bcc) phase formation. Without any stabilizing agent, Zr by itself also phase transforms from α phase to β phase at approximately 850 °C. Hence, the microstructure shows $\alpha + \beta$ structure. This $\alpha + \beta$ structure was also similar to the optical micrographs of a heat-treated Ti-39.6% Zr alloy reported by Farrar et al. [22]. Therefore, the formation of a β phase after laser processing can be attributed to the α -Zr phase powder's melting and solidification process as well as the effect of micro alloying occurring from the Ti6Al4V substrate. Another possibility of the embedded phase would be the formation of intermetallic phases of Ti-Zr, Zr-V, and Zr-Al. However, EDS imaging on these particles, as seen in Figures 5 and 6, showed that the particles were depleted in Al and V. The particles closest to the Ti6Al4V substrate showed low Ti signal on EDS mapping as well. There were also no strong peaks of any intermetallic phase detected by X-ray diffraction. Thus, there is a strong possibility of the formation of a β phase of Zr, which is supported by XRD results and EDS imaging. From Figure 4b,c, it was observed that the diffraction signal was stronger for the samples that had a laser pass on the surface. Thus, the α and β phases of Zr seemed to be more oriented after the laser remelting process.

Laser surface scanning of the LENSTM-deposited Zr had some effect on the hardness of Zr. Hardness increased from 268 HV0.1 to 328 HV0.1. More than the increase in the overall hardness, the drop in hardness in the laser-scanned samples as compared to the sample without any laser scan was more crucial. The hardness dropped from ~328 HV0.1 at a depth of about 0.3 mm to ~220 HV0.1 at a depth of about 1.6 mm. The drop in hardness with increasing depth towards the Ti6Al4V substrate was more gradual in the sample with no laser pass on the surface post-deposition. This can be attributed to the β phase being formed at lower regions near the interface. In the sample with a laser pass, more β phase can be observed at upper regions of the Zr. The particle size of the β phase is also in the range of the length of the diagonals of the indent created during Vicker's hardness testing. On an unetched sample, while doing the hardness testing, different phases cannot be distinguished. Hence, anomalies in the hardness testing can be attributed to the underlying secondary phase particles on which the test was conducted.

The fabrication of a tube-like structure shows the near net shape forming capability of the LENSTM technique applied to reactive materials like Zr. It is possible, therefore, to fabricate functional components out of such reactive materials. It is also possible to make parts with special functional requirements such as porous structure or bimetallic structures. This can be done in a single-step operation and a controlled environment. Other than making functional components entirely out of a single material, important engineering alloys like Ti6Al4V alloy can be selectively coated with reactive materials like Zr.

5. Conclusions

LENSTM, a powder-based additive manufacturing technique, was used to demonstrate the processing of zirconium metal. Zirconium metal powder was deposited on a Ti6Al4V alloy substrate. Some samples were laser-scanned after deposition to cause remelting and solidification of the coatings. The feedstock powder used for processing was completely α -Zr phase. Upon LENSTM processing, both α and β phases evolved. It was found that the laser scanning of the deposited layer increased the orientation of the phases, as indicated by stronger XRD peaks. The grains were equiaxed and there was no change in grain sizes after laser scanning. The hardness of the deposited Zr layers was 268 HV0.1 and increased to 320 HV0.1 after laser scanning. A bulk tube structure was also built to show that LENSTM was successful in processing larger parts of Zr metal. A radial expansion of ~6% was measured compared to the part dimension of the computer-aided design file.

Acknowledgments: The authors acknowledge financial support from the W. M. Keck Foundation to establish the Biomedical Materials Research Laboratory at WSU. The authors also acknowledge financial support from the National Science Foundation under grant number NSF-CMMI 1538851 (PI-Bandyopadhyay).

Author Contributions: This work was done as a part of Himanshu Sahasrabudhe's Ph.D. research at Washington State University under direct supervision of Amit Bandyopadhyay.

Conflicts of Interest: The authors declare no conflict of interest.

References

1. Knittel, D.R.; Webster, R.T. Industrial Application Titanium and Zirconium. In *ASTM Special Technical Publication 728*; American Society for Testing and Materials: Philadelphia, PA, USA, 1979; p. 191.
2. Auchapt, P.; Patarin, L.; Tarnero, M. *Meeting on Fuel Reprocessing and Waste Management*, American Nuclear Society; American Society for Materials: La Grange Park, IL, USA, 1984; p. 2.
3. Nagano, H.; Kajimura, H.; Yamanaka, K. Corrosion resistance of zirconium and zirconium-titanium alloy in hot nitric acid. *Mater. Sci. Eng. A* **1995**, *198*, 127–134. [[CrossRef](#)]
4. Motta, A.T.; Yilmazbayhan, A.; da Silva, M.J.G.; Comstock, R.J.; Was, G.S.; Busby, J.T.; Gartner, E.; Peng, Q.; Jeong, Y.H.; Park, J.Y. Zirconium alloys for supercritical water reactor applications: Challenges and possibilities. *J. Nucl. Mater.* **2007**, *371*, 61–75. [[CrossRef](#)]
5. Albrektsson, T.; Hansson, H.A.; Ivarsson, B. Interface analysis of titanium and zirconium bone implants. *Biomaterials* **1985**, *6*, 97–101. [[CrossRef](#)]
6. Kobayashi, E.; Matsumoto, S.; Yoneyama, T.; Hamanaka, H. Mechanical properties of the binary titanium-zirconium alloys and their potential for biomedical materials. *J. Biomed. Mater. Res.* **1995**, *29*, 943–950. [[CrossRef](#)] [[PubMed](#)]
7. Patel, A.M.; Spector, M. Tribological evaluation of oxidized zirconium using an articular cartilage counterface: A novel material for potential use in hemiarthroplasty. *Biomaterials* **1997**, *18*, 441–447. [[CrossRef](#)]
8. Sahasrabudhe, H.; Bandyopadhyay, A. Additive Manufacturing of Reactive In Situ Zr Based Ultra-High Temperature Ceramic Composites. *JOM* **2016**, *68*, 822–830. [[CrossRef](#)]
9. American Society for Testing and Materials International. *Standard Terminology for Additive Manufacturing Technologies*; ASTM Standard F2792-12a; ASTM International: West Conshohocken, PA, USA, 2012.
10. Krishna, B.V.; Bose, S.; Bandyopadhyay, A. Laser processing of net-shape NiTi shape memory alloy. *Metall. Mater. Trans. A* **2007**, *38*, 1096–1103. [[CrossRef](#)]
11. Balla, V.K.; Bose, S.; Bandyopadhyay, A. Fabrication of porous NiTi shape memory alloy structures using laser engineered net shaping. *J. Biomed. Mater. Res. B Appl. Biomater.* **2009**, *89*, 481–490.
12. Balla, V.K.; Banerjee, S.; Bose, S.; Bandyopadhyay, A. Direct laser processing of a tantalum coating on titanium for bone replacement structures. *Acta Biomater.* **2010**, *6*, 2329–2334. [[CrossRef](#)] [[PubMed](#)]
13. Bandyopadhyay, A.; Tarafder, S.; Balla, V.K.; Bose, S. Laser Processed Tantalum for Implants. *Biomater. Sci. Process. Prop. Appl. II Ceram. Trans.* **2012**, *237*, 123–129.
14. Balla, V.K.; Bandyopadhyay, A. Laser processing of Fe-based bulk amorphous alloy. *Surf. Coat. Technol.* **2010**, *205*, 2661–2667. [[CrossRef](#)]
15. Sahasrabudhe, H.; Dittrick, S.A.; Bandyopadhyay, A. Laser processing of Fe-based bulk amorphous alloy coatings on titanium. *Metall. Mater. Trans. A* **2013**, *44*, 4914–4926. [[CrossRef](#)]
16. Sahasrabudhe, H.; Harrison, R.; Carpenter, C.; Bandyopadhyay, A. Stainless Steel to Titanium Bimetallic Structure using LENS™. *Addit. Manuf.* **2015**, *5*, 1–8. [[CrossRef](#)]
17. Bandyopadhyay, A.; Krishna, B.; Xue, W.; Bose, S. Application of laser engineered net shaping (LENS) to manufacture porous and functionally graded structures for load bearing implants. *J. Mater. Sci. Mater. Med.* **2009**, *20*, 29–34. [[CrossRef](#)] [[PubMed](#)]
18. Balla, V.K.; Bodhak, S.; Bose, S.; Bandyopadhyay, A. Porous tantalum structures for bone implants: Fabrication, mechanical and in vitro biological properties. *Acta Biomater.* **2010**, *6*, 3349–3359. [[CrossRef](#)] [[PubMed](#)]
19. Griffith, M.L.; Schlienger, M.E.; Harwell, L.D.; Oliver, M.S.; Baldwin, M.D.; Ensz, M.T.; Essien, M.; Brooks, J.; Robino, C.V.; Smugersky, E.J.; et al. Understanding thermal behavior in the LENS process. *Mater. Des.* **1999**, *20*, 107–113. [[CrossRef](#)]

20. Murr, L.E.; Martinez, E.; Amato, K.N.; Gaytan, S.M.; Hernandez, J.; Ramirez, D.A.; Shindo, P.W.; Medina, F.; Wicker, R.B. Fabrication of Metal and Alloy Components by Additive Manufacturing: Examplpes of 3D Materials Science. *J. Mater. Res. Technol.* **2012**, *1*, 42–54. [[CrossRef](#)]
21. Bourell, D.L.; Leu, M.C.; Rosen, D.W. *Roadmap for Additive Manufacturing: Identifying the Future of Freeform Processing*; University of Texas: Austin, TX, USA, 2009; Available online: <http://wohlersassociates.com/roadmap2009.html> (accessed on 30 March 2009).
22. Farrar, P.A.; Adler, S. On the System Titanium-Zirconium. *Trans. Metall. Soc. AIME* **1966**, *236*, 1061–1064.



© 2018 by the authors. Licensee MDPI, Basel, Switzerland. This article is an open access article distributed under the terms and conditions of the Creative Commons Attribution (CC BY) license (<http://creativecommons.org/licenses/by/4.0/>).